Compatibility of graphite with primary platinum group metals industrial matte

B. M. Thethwayo* and R. D. Cromarty

Wear resistance of synthetic graphite against liquid industrial platinum group metals furnace matte (Cu–Fe–Ni–S) was investigated from 800°C to 1450°C at a contact time of 1 hour. Graphite resistance was measured by the extent of liquid-matte penetration through the graphite, using X-ray microtomography. The matte was molten at 900°C, and it penetrated through cracks in the graphite wall. The matte penetration depth into the graphite did not increase with temperature. The matte loss in the gas phase increased with temperature. During melting, the volume of the industrial matte expanded. As the matte expanded, it pushed against the wall of the graphite and penetrated through cracks in the graphite wall. Where the crucible volume was large enough to accommodate the expanded matte, the matte did not penetrate through the graphite. Graphite exhibited poor resistance against penetration by the liquid industrial platinum group metals furnace matte.

Keywords: PGM-smelter, PGM-matte, Graphite, Matte penetration, Refractories

Introduction

Application of carbon-based refractories is a recent development in the refractory-wall design of platinum group metals (PGM) smelters. Graphite blocks are currently used as a barrier between the copper coolers and the hot furnace melt at the slag–feed level of PGM smelters.[1] Graphite has improved the integrity of PGM furnace linings in the slag–feed tidal zone.[2] It is believed that using graphite in the matte zone might improve the service life of PGM smelter refractory linings. Previous work has focused on assessing the compatibility of graphite with a synthetic matte. Although the synthetic matte did not penetrate through the graphite, matte loss of up to 5 wt-% was observed.[3] This work aimed to examine the compatibility of liquid industrial PGM furnace matte with RN graphite at typical matte operating temperatures. The matte penetration depth was used as a measure of the graphite refractory compatibility with the liquid matte. The experiments performed aimed to address the following research questions.

Does liquid industrial PGM furnace matte (Cu–Fe–Ni–S) penetrate through uncooled RN graphite? Does the operating temperature affect the rate at which the matte penetrates through the graphite? Research hypothesis: 'Penetration depth of industrial matte through graphite increases with operating temperature at constant contact time'.

The temperature of the interaction between the melt and the refractory is an important factor in determining the corrosion rate of a refractory.[4] Penetration, dissolution and spalling are important phenomena that control the corrosion of industrial refractories.[5] Penetration is the focus of this study, and can be categorised into physical penetration and chemical invasion. Physical penetration is when a non-wetting liquid is forced into the pores of a solid through external forces. Chemical invasion is when there is dissolution and penetration occurs.[5] Penetration is favoured by low-viscosity liquids.[5] For a sulphide mixture (Cu_2S, FeS, Ni_3S_2), viscosity depends on the amount of FeS in the mixture.[6] For a sulphide mixture with FeS of <80 wt-%, viscosity decreases with temperatures between 1100 and 1500°C.[6] The average FeS content in the tested matte was 66 wt-%; therefore, the viscosity of the matte was expected to decrease with the operating temperature. For this reason, the depth of the matte penetration into the graphite should increase with increasing operating temperatures.

Materials and methods

The RN graphite

The RN graphite tested was acquired from Sigri Great Lakes Carbon Company (SGL) and was a typical graphite grade used as a hot face refractory lining in the slag–feed zone of an industrial PGM smelter. The grade name for the graphite used is "RN". The RN graphite had 24% porosity, 1.62 g cm^{-3} density and a thermal conductivity of $150 \text{ W m}^{-1} \text{ K}^{-1}$. It was an extruded material and for this reason it has manufacturing defects such as cracks. The RN graphite was, however, an economical material for use as a refractory because of its comparatively low cost.

Department of Material Science and Metallurgy, University of Pretoria, Centre for Pyrometallurgy, Pretoria, South Africa
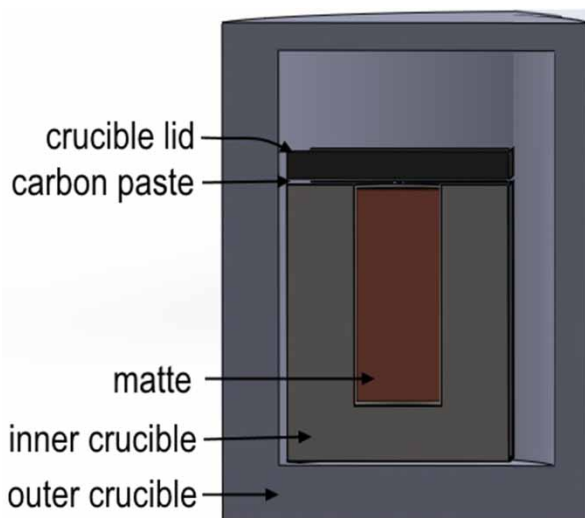
*Corresponding author, email 77mpilot@gmail.com

Industrial PGM matte

The industrial PGM matte (Matte A) tested was acquired from the Waterval smelter of Anglo platinum (Amplats) and was granulated during tapping. Matte A was analysed with electron probe microanalyser–wavelength-dispersive spectroscopy (EPMA–WDS) to determine its chemical composition. Iron sulphide, iron–nickel alloy and iron–copper–nickel sulphide (solid solution) were major sulphide phases detected in the obtained matte. There were oxide inclusions in the matte which consisted of iron chromium oxide and silicates of iron, iron magnesia and calcium alumina. The obtained matte was subjected to X-ray fluorescence (XRF) to determine its bulk elemental composition. The proportions of the base metals (Cu, Fe, Ni, Co and Cr) in Matte A were comparable with the published data of furnace matte composition from the Waterval smelter (reported by Jones). [7] The sulphur content of Matte A was relatively lower than the published 27 wt-%, and this may be attributed to the presence of the impurities that were detected. Appreciable amounts of impurities, such as Si, Mg, Al and Ca, were detected by XRF in Matte A. The XRF and EPMA analyses were in agreement as both techniques detected the slag elements in the matte. The presence of slag impurities in Matte A was somewhat unexpected since the oxide phases typically collect in the slag phase during industrial PGM matte smelting. Slag entrainment and slag dissolution in matte are typical phenomena in the PGM matte smelting process[8] that can lead to high amounts of slag components in matte. The obtained Matte A had up to 5 wt-% oxide phases.

Analytical techniques

X-ray microtomography (XRM) is a non-destructive technique which uses X-rays to cut a specimen digitally to reveal its interior details.[9] Tomography measures a projection of the attenuation coefficients. The specimen is scanned with X-rays after which digital geometry processing is used to generate a three-dimensional (3D) image of the scanned object.[9–11] A computerised reconstruction of the sample is then carried out.[10] Grey levels in a computed tomography image (tomogram) correspond to X-ray attenuation which is a function of X-ray energy, density and atomic number of the material being analysed.[11] Material with a high density and atomic number appear brighter than material with a low density and atomic number.

Errors because of sample cutting and polishing are eliminated with tomography analyses since the specimen is analysed as is. The 3D feature of the XRM allows visual layout of the inside of the specimen without cutting open the specimen. It gives a detailed and more accurate analysis of the specimen layout than a 2D view which only gives a view from one plane. The disadvantage of using XRM is the lack of detectors to acquire chemical composition of different phases.

Scanning electron microscopy (SEM) (JEOL JSM6300 and SEM5800) was used for sample characterisation. The SEM uses energy-dispersive spectrometry (EDS) and back-scattered electron (BSE) detectors. The EDS measures the counts and energy of X-rays emitted by the specimen. It is used to determine the elemental composition of samples. The BSE measures the fast electrons emitted by the specimen.[12] The BSE was used for phase identification.

An EPMA was used to determine the chemical composition of the phases in the samples. The EPMA was fitted with a WDS detector which measured the wavelengths of the X-rays emitted by the specimens.[12]

Experimental methods

Crucible tests were performed to assess the resistance of the RN graphite to penetration by the liquid industrial PGM matte. A graphite block was cored out to create a crucible. A typical crucible specimen is shown in Fig. 1. The as-received matte was milled to ground powder and weighted into the graphite crucible. The matte-filled crucible was closed with a lid; carbon paste was applied between the crucible and the lid to ensure a tight seal. The graphite–matte specimen was enclosed in a graphite crucible to prevent contamination of the specimen and to capture any material that might penetrate through the inner crucible. The operating temperature was varied from 800 to 1450°C. The minimum operating temperature (800°C) was selected based on the liquidus temperature of matte (850°C).[13] The highest operating temperature (1450°C) was limited by the equipment

1 Graphite–matte specimen set-up, a cross-section
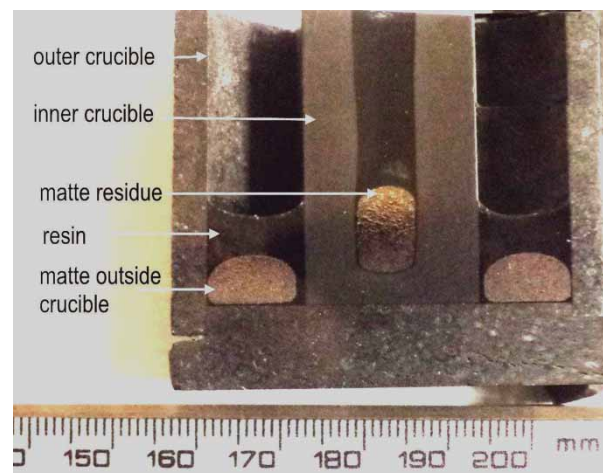
2 Graphite–matte specimen after 1 hour exposure at 1450°C, a cross-section

used which cannot run above 1500°C. A vertical tube furnace was used to heat the specimen. The heating and cooling rate was 4°C per minute. The specimen was held at temperature for 1 hour after which it was cooled to 50°C. Purified argon gas was used to purge the furnace to prevent oxidation of the specimen during the experiment.

Results and discussion

The layout of the specimen after exposure is shown in Fig. 2. The matte started melting at 900°C, and molten matte penetrated through the graphite at 900°C (at 800°C the matte was solid). A portion of the matte was collected outside the crucible in a solid form (matte outside crucible is shown in Fig. 2), while a proportion of the matte remained inside the crucible after exposure (matte residue is shown in Fig. 2). The observation of the solid matte outside the crucible indicated that the liquid matte penetrated through the RN graphite during exposure. The graphite–matte specimen was subjected to XRM and SEM–BSE to determine the penetration path of the matte through the RN graphite crucible.

The XRM analyses

The XRM was used to acquire the layout of the graphite–matte specimen after exposure. Photon energy of 100 kV and beam energy of 7 W were used to analyse the specimen.

The matte seemed molten and highly porous at 900°C. A top view image of a graphite–matte specimen at 900°C is shown in Fig. 3. Matte adherence to the graphite surface is apparent. Slag phases can be seen dispersed in the matte. Traces of matte can be observed in the cracks of the graphite wall from the matte–graphite interface to the outer surface of the graphite.

The micrograph of a specimen after exposure at 1250°C is shown in Fig. 4 (Fig. 4a is a 3D image and Fig. 4b is a 2D image). A 3D image shows that matte penetration in the graphite was observed throughout the width of the crucible. A 2D image only shows a few spots of matte traces in the wall of the graphite. The contrast between the 3D and 2D images highlights the advantage of the XRM technique. Relying on one plane view (2D image) of the specimen may result in misleading conclusions from the analysis. A thin layer of matte was observed attached to the graphite surface from the crucible lid to the bottom of the crucible where a dense matte layer had collected. A thin layer of a slag phase could be observed on top of the matte layer. Traces of matte could be seen through the lid and the walls of graphite. Matte was observed on the outer surface of the crucible (MOC (Matte which penetrated through the crucible_Matte Outside the Crucible) in Fig. 4), and matte could be traced back to the inside of the crucible using traces of matte in the wall of the crucible. This was a typical example of how matte gets out of a crucible.

The matte seemed fully molten at 1450°C and a metallic phase had formed and settled below the matte layer. Matte had detached from the graphite surface and the top part of the crucible had no matte attached to the surface such as observed at 900 and 1250°C. The pores observed in matte at low temperatures were significantly decreased at 1450°C. The oxide phases (impurities) had reacted with the matte, forming sulphide phases enriched in Al, Ca, Cr, Mg and Si. The residual oxide phases had collected on top of the matte. Traces of matte could still be observed on the wall of the graphite, mostly in the bottom portion of the wall.

Solid matte observed in the walls of the crucible indicated that the path through which the matte penetrated out of the crucible was the cracks and pores present in the walls of the as-received graphite. Traces of matte
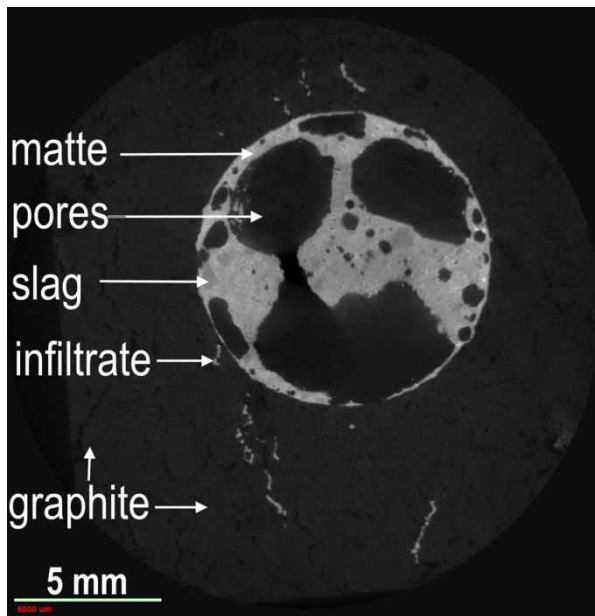
3 Graphite–matte specimen after 1 hour exposure at 900°C, top view image by XRM
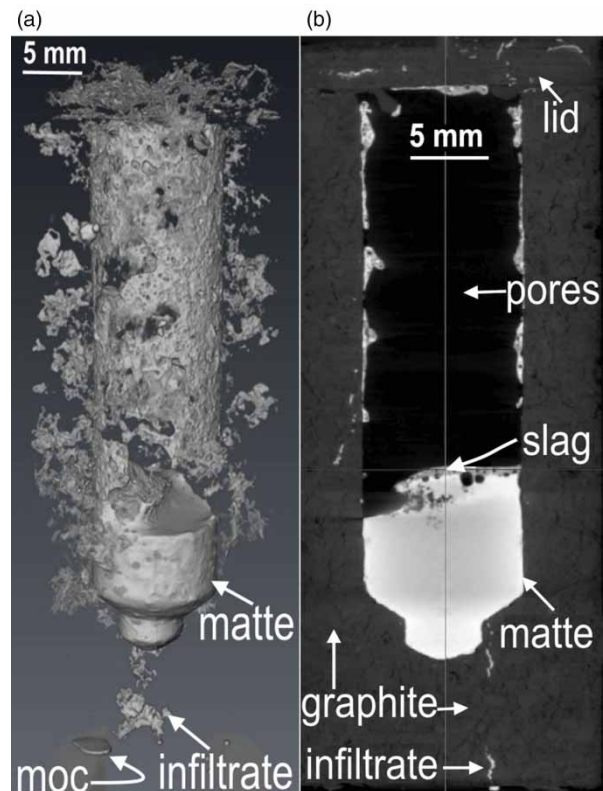
4 Graphite–matte specimen after 1 hour exposure at 1250°C: a 3D; b 2D side view images by XRM

were more prevalent in the cracks of the crucible wall than in the pores. Traces of matte were not observed between the lid and the crucible where a carbon paste was applied; this meant the carbon paste successfully prevented matte penetration between the lid and the crucible. The XRM analyses of the specimen showed that matte penetrated through the entire width of the graphite crucible wall and reached the outer surface of the crucible, as seen in Fig. 4.

Possible mechanisms causing industrial matte penetration through the RN graphite

Changes in matte properties during melting (expansion of matte volume)

The volume of the industrial matte increased substantially during melting at temperatures between 900 and 1000°C. Wettability tests performed as part of this study revealed that the volume of the industrial matte expanded by up to 25% of the original size. Matte expansion could occur as a result of a change in cell units of matte species owing to phase transformation that occurs during the melting of sulphides. To determine the effect of the matte expansion on the matte penetration through the graphite, tests were conducted in which the level or volume of the matte in the graphite crucibles was varied. One crucible was filled with matte to capacity, as in Fig. 1; the other crucible was half-filled with matte. The matte-filled graphite crucibles were heated to 1150°C and held for 1 hour. The crucibles that were half-filled with matte were not penetrated by liquid matte (no matte was observed outside the crucible after exposure). The crucibles that were filled to full capacity were penetrated by the liquid matte. The penetrated matte was around 50 wt-%, as observed in tests performed at 900°C. The penetration rate of the matte through the graphite proved to be independent of the operating temperature and exposure time. It seemed that the proportion of liquid matte that penetrated through the crucible was correlated with the extent to which the crucible volume could accommodate the expanded matte. In a half-filled crucible, there was enough volume inside the crucible to accommodate the expanding matte until it reached the stable volume without increasing the pressure inside the crucible to a point where the matte was forced out of the crucible. In a full crucible, there was no space inside the crucible to accommodate the expanded matte and for this reason, pressure accumulated inside the crucible to a point where the molten matte found cracks and pores in the graphite wall through which the matte penetrated out of the crucible. When the matte reached a constant volume, the matte expansion ceased and the matte penetration stopped. This was based on the fact that the liquid matte penetration in a full crucible averaged around 50 wt-%, irrespective of the operating temperature. In an industrial smelter, sulphides start melting at the feed–slag interface after which matte falls through the slag and settles below the slag layer.[8] The effect of matte expansion is not a factor in an industrial smelter since there is enough space inside the furnace to accommodate changes in the volume of the matte.

Hydrostatic pressure [$P = \rho g h$]

For a static fluid with constant specific weight, pressure varies only with the elevation within the fluid.[14] Pressure increases with depth in a fluid. The hydrostatic pressure equation is shown in equation (1), where ρ is the density of the fluid in kg m^{-3}, g is the acceleration gravity (9·81 m s^{-2}) and h is the depth of the fluid in meters.[14] The hydrostatic pressure cannot be the main mechanism by which matte penetrates through the graphite in the current work since the crucible height was about 40 mm; the pressure drop from the lid to the bottom of the crucible is minimal.

$$
\begin{aligned}
P &= \rho g h \\
&= \rho_{\text{feed}} \times g \times h_{\text{feed}} \ + \ \rho_{\text{slag}} \times g \times h_{\text{slag}} \ + \rho_{\text{matte}} \\
&\quad \times g \times h_{\text{matte}}
\end{aligned}
\tag{1}
$$

In an industrial application, hydrostatic pressure cannot be ignored since the matte zone is at the bottom of the furnace. Therefore, the head pressure is the highest in the matte zone. An estimation of the hydrostatic pressure in a typical industrial smelter was done using the PGM bath properties extracted from Eksteen.[8] The density of a PGM feed varies from 1300 to 1600 kg m^{-3}, and its height varies from 200 to 400 mm. Slag density varies from 3800 to 4200 kg m^{-3}, and its height varies from 800 to 1100 mm. Matte density varies from 4800 to 5200 kg m^{-3}, and its height varies from 200 to 300 mm. Based on these values, the estimated minimum and maximum pressures at the bottom of a matte level is 0·390 and 0·660 atm., respectively, while the pressure at the slag–matte interface varies from 0·320 to 0·510 atm.

Based on the estimated static fluid pressure in the matte level of a typical industrial smelter, the effect of static fluid pressure in the industrial smelter seems substantial. The static fluid pressure can cause the liquid matte to penetrate through the cracks in the graphite blocks or spaces between graphite blocks (graphite block interface).

Evaporation of volatile matte species

The formation of high volumes of gases is envisaged during melting of industrial base metal sulphides.[8] The vaporisation of matte species results in a loss of matte to a gas phase. The increase of the volume of the gas inside the crucible creates pressure that will drive the gas to escape the crucible. During the current experiments, a gas condensate accumulated in the cooled portion of the furnace work tube. The gas condensate consisted of copper iron sulphide phases and silicon disulphide (SiS$_2$). These elements were constituents of the matte, which indicated that matte evaporates during exposure to high temperatures; up to 5 wt-% matte could not be accounted for after exposure. Although matte loss to a gas phase is an occurrence, its impact is not significant when compared with the liquid matte penetration, which can amount to 50 wt-% of the matte.

Chemical reactions between matte and graphite

The composition of the matte that penetrated through the crucible and the matte that remained inside the crucible was similar. Iron sulphide, iron–copper sulphide, iron–copper–nickel sulphide solid solution and iron–nickel alloy were major phases detected in the matte residue. The oxide phases remained inside the crucible. The slag has a higher liquidus temperature (1450–1500°C)[13] compared with that of matte (875°C).[8] Therefore, at 900°C the slag phases should still be solid which would hinder the slag phases penetration with the molten matte out of the crucible. Consumption of graphite at the

graphite–matte interface seemed minimal; no significant change in the dimensions of the graphite was observed. Carbon pick-up by the matte was up to 0·1 wt-% after exposure; this was considered minimal. Chemical reactions could therefore not be the main mechanism by which matte penetrated through the graphite crucible.

Penetration of liquid matte through the graphite would have detrimental results in an industrial application since the cold face of the refractory of the PGM smelter is lined with copper blocks. Copper blocks are susceptible to sulphur-containing gases and molten sulphides, and therefore copper blocks should not come in contact with these species. The hot face of the refractory would have to be sufficiently cooled to below the liquidus temperature of the melt to freeze the melt before it reached the surface of the copper coolers.

Conclusion

The penetration of liquid matte through RN graphite was not significantly affected by the operating temperature. Industrial matte penetrated through graphite as it began melting at 900°C. During the melting of sulphides, significant expansion of the volume of the matte was observed. Penetration of matte through the graphite was driven by pressure build-up inside the crucible that resulted from matte expansion and gas evolution during the melting of sulphides. A crucible half-filled with matte was not penetrated by liquid matte, while a fully filled crucible was penetrated by liquid matte. Increasing the operating temperature enhanced the matte loss to the off-gas. The hypothesis 'Penetration depth of industrial matte through RN graphite increases with operating temperature at constant contact time' was proven null. The liquid penetration of matte through the graphite crucible was not enhanced by an increase in operating temperature.

Acknowledgements

References

1. P. K. Van Manen: 'Furnace energy efficiency at Polokwane smelter', Third Int. Platinum Conf. 'Platinum in Transformation', Sun City, SA, 2008, SAIMM, 191–196.
2. B. M. Thethwayo: 'Sulphidation of copper coolers in PGM smelters', MSc thesis, University of Pretoria, SA, 2010.
3. B. M. Thethwayo and A. M. Garbers-Craig: 'Interaction of graphite with synthetic matte', In Proc. 5th Int. Platinum Conf. on 'A catalyst for change', Suncity, South Africa, 18–20 September 2012, SAIMM, 261–274.
4. V. K. Pavlovskii and Y. S. Sobolev: 'Effect of temperature on the corrosion of refractories in glass melts (review)', *Glass Ceram.*, 1991, **48**, (12), 558–561.
5. M. Rigaud: 'Corrosion of refractories and ceramics'. in 'Uhlig's corrosion handbook', (ed. R. W. Revie), 3rd edn., 387–398; 2011, Hoboken, NJ, Wiley.
6. W. Sundström, J. J. Eksteen and G. A. Georgalli: 'A review of the physical properties of base metal mattes', *J. SAIMM*, 2008, **108**, 431–448.
7. R. T. Jones: 'Platinum smelting in South Africa', *South Afr. J. Sci.*, 1999, **95**, 525–534.
8. J. J. Eksteen: 'A mechanistic model to predict matte temperatures during the smelting of UG2-rich blends of platinum group metal concentrates', *Miner. Eng.*, 2011, **24**, (7), 676–687.
9. M. Holler, A. Diaz, M. Guizar-Sicairos, P. Karvinen, E. Färm, E. Härkönen, M. Ritala, A. Menzel, J. Raabe and O. Bunk: 'X-ray ptychographic computed tomography at 16 nm isotropic 3D resolution', Scientific Reports, 4, 2014, doi:10·1038/srep03857.
10. N. Dhawan, M. S. Safarzadeh, J. D. Miller, M. S. Moats, R. K. Rajamani and C. L. Lin: 'Recent advances in the application of X-ray computed tomography in the analysis of heap leaching systems', *Min. Eng.*, 2012, **35**, 75–86.
11. R. A. Ketcham and W. D. Carlson: 'Acquisition, optimization and interpretation of x-ray computed tomographic imagery: applications to the geosciences', *Comput. Geosci.*, 2001, **27**, (4), 381–400.
12. J. Goldstein, D. E. Newbury, D. C. Joy, C. E. Lyman, P. Echlin, E. Lifshin, L. Sawyer and J. R. Michael: 'Scanning electron microscopy and X-ray microanalysis', 1/10–1/18, 3/75–3/96; 2003, New York, NY, Springer.
13. J. J. Eksteen, B. Van Beek and G. A. Bezuidenhout: 'Cracking a hard nut: an overview of Lonmin's operations directed at smelting of UG2-rich concentrate blends', *SAIMM*, 2011, **111**, (10), 681–690.
14. C. T. Crowe, D. F. Elger and J. A. Roberson: 'Engineering fluid mechanics', 8th edn, 35–64; 2005, Hoboken, NJ, Wiley.